

Adsorption of molecules zinc oxide (ZnO) and iron disulfide (FeS₂) on the surfaces of (Li₁₀C₁₀) and (Li₁₅C₁₅) utilizing DFT

Hanaa Mohammed Hadad^{1*}, Abbas Shwya Alwan²

^{1,2}Physics Department, College of science, Thi-Qar University, Thi-Qar, Iraq; Hanaa.m.hadad@utq.edu.iq (A.S.A.)

abbasshwa_ph@sci.utq.edu.iq (H.M.H.)

Abstract: The density functional theory (DFT) has been submitted with the basis sets 6-31G, B3LYP at the level of the ground state by utilizing sophisticated algorithms in the Gaussian09 program in order to investigate the molecular structure, electrostatic potentials (ESP), infrared spectra (IR), contour curves, and density of states (with the Gauss Sum 03 package) for the nanomaterials Li₁₀C₁₀, Li₁₀C₁₀ZnO, Li₁₀C₁₀FeS₂, Li₁₅C₁₅, Li₁₅C₁₅ZnO, and Li₁₅C₁₅FeS₂. Using similar methodologies, the electronic properties: HOMO energy, SOMO energy, LUMO energy, energy gap (E_g), polarizability, dipole moment (μ), electron affinity, ionization potential, and symmetry have been calculated. The distribution of charge density concentrates around some atoms in the samples under study more than others due to the constraints of quantum mechanics and Fermi-Dirac statistics of the fermions (here, the electrons). Electrostatic potential images and contour curve diagrams demonstrate an increase in charge density in the adjacent regions between zinc, sulfur, oxygen, and carbon lithium nanomaterial surfaces, confirming the adsorption process of those atoms on the carbon lithium nanomaterial surfaces. Infrared spectra reveal the appearance of new peaks corresponding to new bonds, such as Zn-C and Fe-C, confirming the occurrence of the adsorption phenomena of iron and zinc on the nanomaterial surfaces (Li₁₀C₁₀) and (Li₁₅C₁₅). The numerical values of energy gaps (E_g) of the nanomaterials under study fall within the range of numerical values typical of semiconductors, which is considered highly advantageous for applications in electronics, such as p-n junctions and solid-state lasers. The adsorption process of zinc oxide on lithium carbon nanomaterial surfaces increases the value of polarizabilities, which is very important in the field of nonlinear optics applications, such as telecommunications and internet networks.

Keywords: Adsorption, Density of states DFT, Energy gap, Infrared spectra (IR), SOMO.

1. Introduction

Quantum mechanical techniques like the Hartree-Fock approximation, post-Hartree-Fock methods, and density functional theory can be utilized to study the electronic structure of specific atoms, molecules, nanomaterials, nanoribbons and substances [1]. The many body systems calculations could be carried out throughout the electron density function with accordance to density functional theory (DFT) rather than the wave function [2]. Electron density function typifies the probability of identifying the locations of electrons at a given space [3]. The wave function approximation takes into account 3N variables, three spatial coordinates, and one coordinate for spin under the presumption that the location of the nuclei is fixed, whereas density functional theory assumes that the electron density depends only on three spatial coordinates and does not take into account how the electrons are found in the systems [4]. Density functional theory (DFT) allows one to determine the credits of a many electron system throughout the functionals. The functionals are functions of another functions [5]. One of the most widely utilized techniques in computational physics and chemistry for determining the

electronical characteristics of solid state nanomaterials is the density functional theory (DFT) [6]. For solid state systems, the results of density functional theory (DFT) calculations are closely matching the experimental data [7]. Hohenberg and Kohn proposed density functional theory in two seminal papers were published in 1960s [8]. However, density functional theory (DFT) had not been regarded accurate enough in quantum chemistry calculations until 1990s [5]. The density functional theory (DFT) aims to calculate the energy of the N electron system's ground state based on its density function rather than the wave function [9]. John Pople and Walter Kohn shared the 1998 Nobel Prize in Chemistry. Pople utilizes concepts of quantum chemistry and quantum physics to build density functional theory (DFT) Computationally [5]. In 2001 a hybrid lithium ion capacitor successfully developed by a research team [10]. Many studies were conducted to enhance the performance of electrodes and electrolytes, in 2010 Naoi et al. discover a nanostructure composite of carbon nanofibers and lithium titanium oxide (LTO) [11]. Since sodium is far less expensive than lithium, the sodium ion capacitor (NIC) currently occupies another area of attention. However, it is now not economically viable because the LIC continues to overcome the NIC. Many applications are providing high energy and high power can utilize lithium-ion capacitors. They save money by eliminating the need for extra electrical storage devices in a variety of applications because they combine high energy and high power. Some applications for lithium-ion capacitors are photovoltaic power generation and energy recovery systems in industrial machinery [12]. Application of carbon nanomaterials as an anode or one of the components of anodes based on lithium tend to improve sulfur lithium ion with high energy density lithium ion disulfur (Li-S) batteries [13]. Modern sophistications in lithium ion batteries that depend on carbon nanomaterials have been presented in order to improve energy sources [14]. Sophistications carbon nanomaterials save a chance to improve new nanomaterials for energy storage that have been applied in lithium ion batteries [15].

The study aims to find nanomaterials own importance in the applications in the manufacture of electronic devices such as sensors, solar cells pieces of laptops. Either one of the most important points that the research seek on, is finding nanomaterials may be utilized in the future in the energy storage devices such as the capacitors.

2. Results and Discussion

2.1. Molecular Structure

The molecular geometry implies systemization of atoms through the molecule. The molecular structure gives beneficial information for determination the important properties of the molecule, like, the magnetic properties and polarizability [16, 17]. The molecular geometry for the nanomaterials $\text{Li}_{10}\text{C}_{10}$, $\text{Li}_{10}\text{C}_{10}\text{ZnO}$, $\text{Li}_{10}\text{C}_{10}\text{FeS}_2$, $\text{Li}_{15}\text{C}_{15}$, $\text{Li}_{15}\text{C}_{15}\text{ZnO}$ and $\text{Li}_{15}\text{C}_{15}\text{FeS}_2$. DFT have been carried out throughout utilizing density functional theory (DFT) with the hybrid functional B3LYP and the basis set 6-31G at the ground state level.

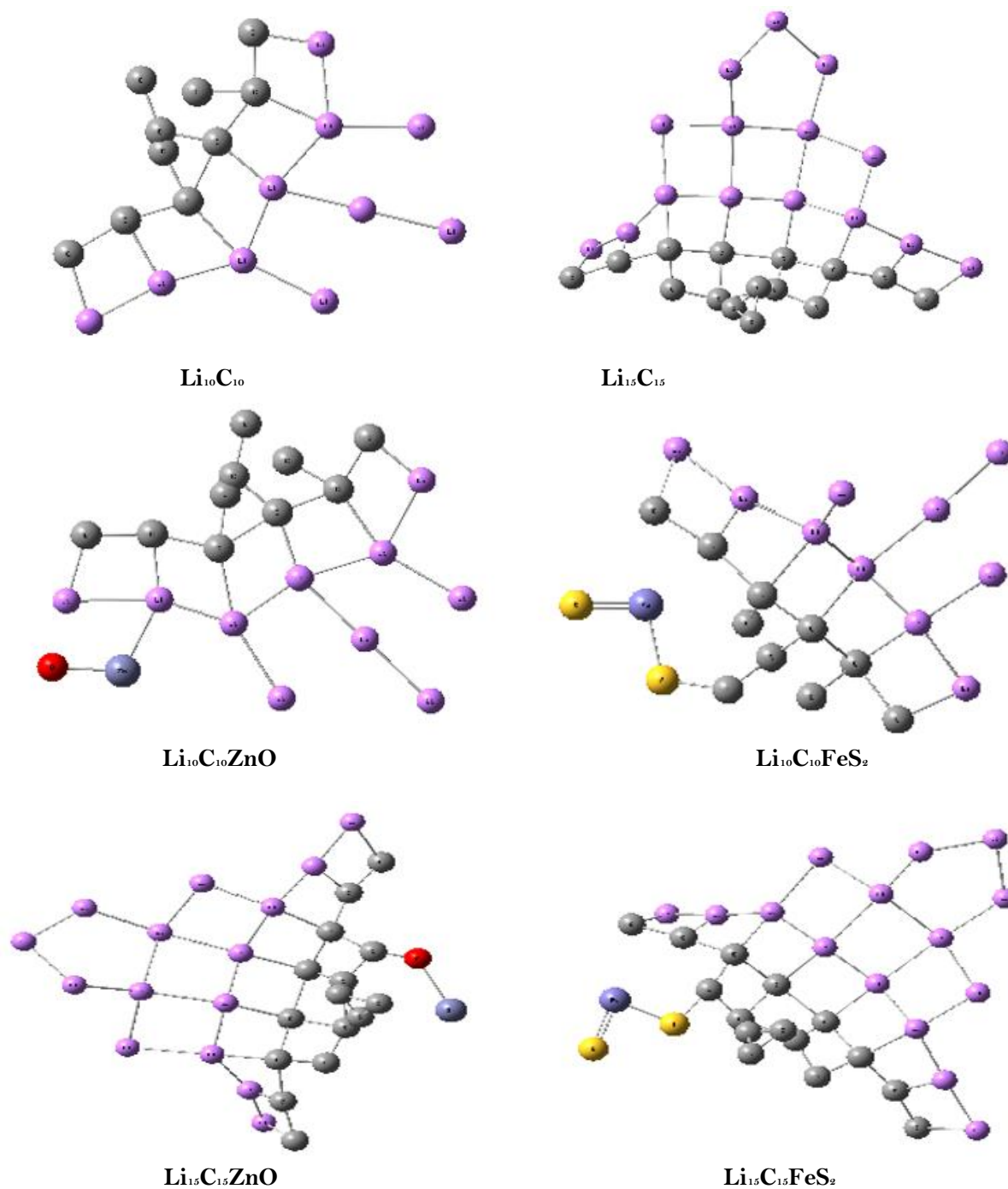


Figure 1.
Molecular geometry for Li₁₀C₁₀, Li₁₀C₁₀ZnO, Li₁₀C₁₀FeS₂, Li₁₅C₁₅, Li₁₅C₁₅ZnO and Li₁₅C₁₅FeS₂.

Figure 1 demonstrate the lithium atoms with violet color, the carbon atoms with lead color, the iron atoms with light blue color, the disulfur atoms with yellow color, the zinc atoms with blue light lead but the oxygen atoms with red color. When an atom close to other atom, the energy level split into two levels, the electrons occupy the energetic levels. When number of atoms N close together the

energy levels split into N energetic levels, then, the energy bands will generate, the electrons will take its position in energy bands. Studying the molecular structure consider very necessary because understanding the molecular structure help to understand the designation mechanics and the complicated diagrams in the nature. Practically the molecular structure can be examine by electrons diffraction, infrared spectra or X-ray diffraction. The molecular structure demonstrates the special configuration of the atoms in Cartesian coordinates (x, y, z) . The distance between each two atoms ought to equal to the atomic radius of the two atoms, but sometimes the distance is not the same because of many actors, just like, molecular bonding, hybridization and symmetry.

2.2. *Electrostatic Potential (ESP)*

HOMO, LUMO and SOMO surfaces give a description to the electrostatic potential. Geometrically the surface typifies a shape with two dimensions, they are length and width but no thickness. According to solid state physics the surface means the first three layers of the material. The molecular orbitals originate as a result to the linear combination of the atomic orbitals according to the molecular orbital theory [18, 19]. The electrostatic potentials (ESP) for the nanomaterials $\text{Li}_{10}\text{C}_{10}$, $\text{Li}_{10}\text{C}_{10}\text{ZnO}$, $\text{Li}_{10}\text{C}_{10}\text{FeS}_2$, $\text{Li}_{15}\text{C}_{15}$, $\text{Li}_{15}\text{C}_{15}\text{ZnO}$ and $\text{Li}_{15}\text{C}_{15}\text{FeS}_2$. DFT have been carried out throughout utilizing density functional theory (DFT) with the hybrid functional B3LYP and the basis set 6-31G at the ground state level.

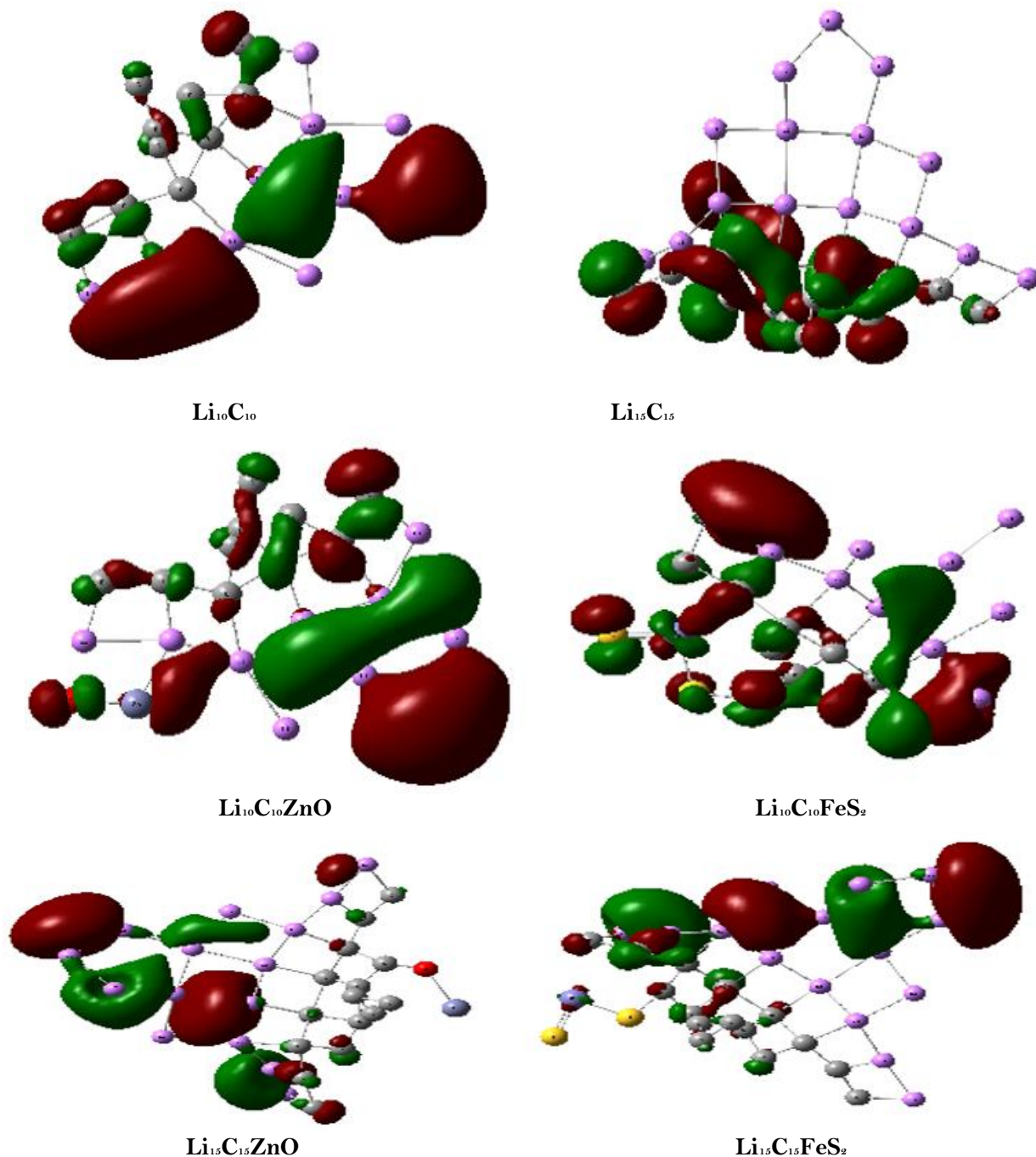


Figure 2.

The electrostatic potential surface (ESP) for Li₁₀C₁₀, Li₁₀C₁₀ZnO, Li₁₀C₁₀FeS₂, Li₁₅C₁₅, Li₁₅C₁₅ZnO and Li₁₅C₁₅FeS₂.

Figure 2 demonstrates apparently impact of the adsorption procedure to the electrostatic potentials surface. One can visualize the dissimilarity in the electronic charge distributions around the atoms. Pictures of electrostatic potential surface depicts distribution of the density of electronic charges around the positive cores. The nucleus is founded in the centers of atoms and it stand for the positive cores. The electronic cloud surround the positive cores. One can imagine the nuclei set test positive charge to attract the electrons. One can see in the pictures of electrostatic potentials new colors red and green, the

red color typifies the minimum value of the potential, but the green color typifies the maximum value of the potential. A simplified comparison between $\text{Li}_{10}\text{C}_{10}$ and $\text{Li}_{10}\text{C}_{10}\text{FeS}_2$ clarifies that the iron atom and disulfur atoms adsorbed on carbon atoms. A simplified comparison between $\text{Li}_{10}\text{C}_{10}$ and $\text{Li}_{10}\text{C}_{10}\text{ZnO}$ clarifies that zinc atoms and oxygen atoms adsorbed lithium atoms. The comparison between $\text{Li}_{15}\text{C}_{15}$ and $\text{Li}_{15}\text{C}_{15}\text{FeS}_2$ demonstrate the charge distribution in the nanomaterial structure $\text{Li}_{15}\text{C}_{15}$ around carbon atoms be more than lithium atoms, but the charge distribution in the nanomaterial structure $\text{Li}_{15}\text{C}_{15}\text{FeS}_2$ around lithium atoms be more than carbon atoms. The reason here that the electronic charges distribution subjects to the restrictions of quantum mechanics and Fermi-Dirac statistics.

2.3. Contours

The electronic density curves the electronic charge density around the atoms in the geometrical structure. Also contours express Fermi level and Fermi energy. The active locations in the contour structure point out concentration of electronic charge distribution in this locations. Therefore, contours show electronic charge distribution around the atoms and the active regions in this distribution [20, 21]. The electronic density contours for the nanomaterials $\text{Li}_{10}\text{C}_{10}$, $\text{Li}_{10}\text{C}_{10}\text{ZnO}$, $\text{Li}_{10}\text{C}_{10}\text{FeS}_2$, $\text{Li}_{15}\text{C}_{15}$, $\text{Li}_{15}\text{C}_{15}\text{ZnO}$ and $\text{Li}_{15}\text{C}_{15}\text{FeS}_2$. DFT have been carried out throughout utilizing density functional theory (DFT) with the hybrid functional B3LYP and the basis set 6-31G at the ground state level.

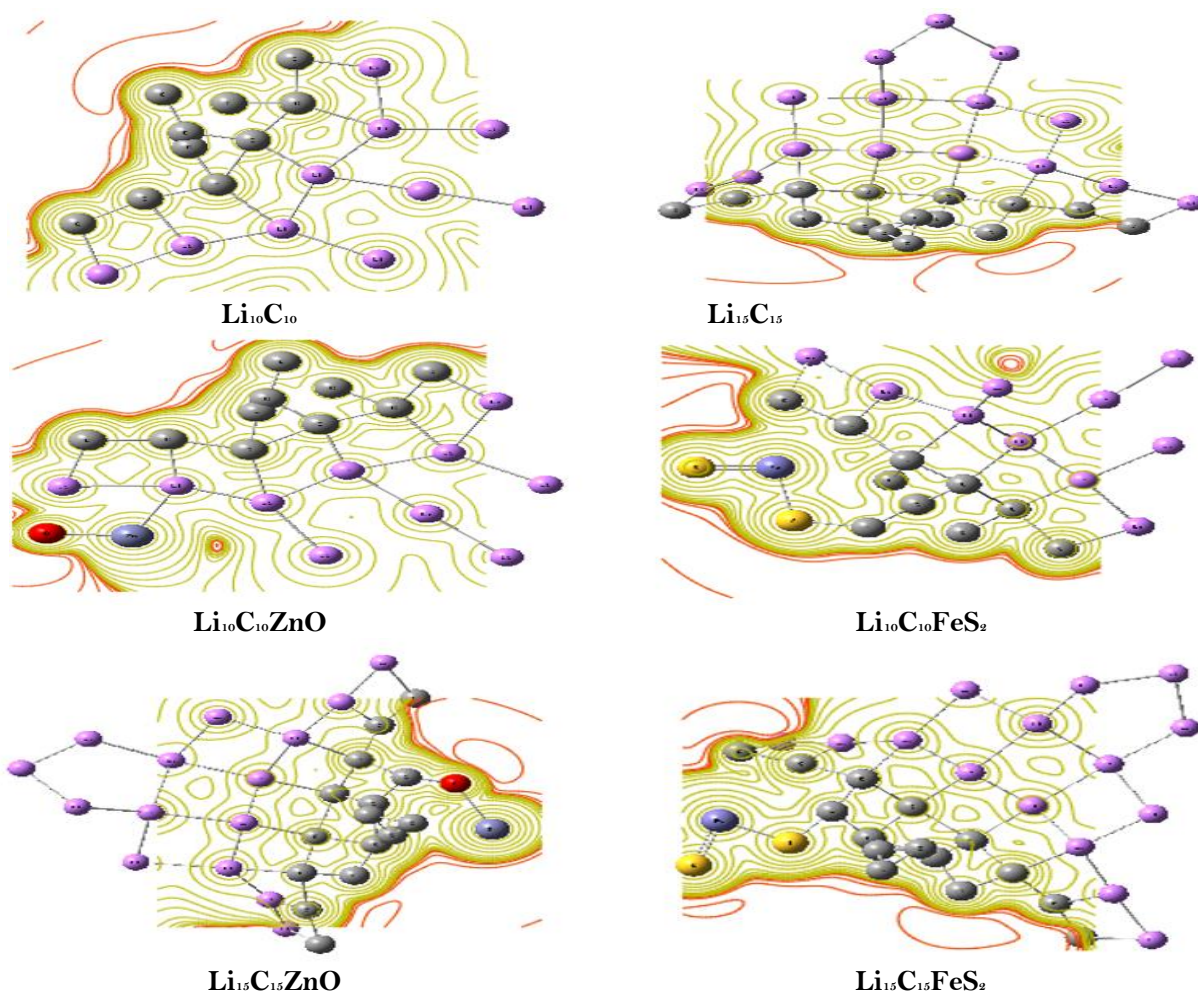


Figure 3.

The contour density maps for $\text{Li}_{10}\text{C}_{10}$, $\text{Li}_{10}\text{C}_{10}\text{ZnO}$, $\text{Li}_{10}\text{C}_{10}\text{FeS}_2$, $\text{Li}_{15}\text{C}_{15}$, $\text{Li}_{15}\text{C}_{15}\text{ZnO}$ and $\text{Li}_{15}\text{C}_{15}\text{FeS}_2$.

Figure 3 exhibits the adsorption procedure of zinc oxide on the nanomaterial surfaces $\text{Li}_{10}\text{C}_{10}$ and $\text{Li}_{15}\text{C}_{15}$, because the electronic charge distribution in the contour curves concentrates near the adjacent regions between zinc oxide and $\text{Li}_{10}\text{C}_{10}$, so the electronic charge distribution in the contour curves concentrates near the adjacent regions between zinc oxide and $\text{Li}_{15}\text{C}_{15}$. Contour density maps typify a tool for representation the three dimension surface in two dimension. Contour density maps here give a description to the adsorption procedure that originate as a result to the interaction of zinc, oxygen and disulfur with the carbon lithium nanomaterial surfaces. Also contour density maps show apparently Brillion zones. The allowed regions to be occupied by electrons or to be forbidden are determined throughout Brillion zones. The vacancies between Brillion zones typifies the forbidden regions to be occupied by the electrons. The Brillion zone is very important concept in the physics of solids. One can visualize in the pictures of density contour maps that charge concentration in the nanomaterial structure $\text{Li}_{15}\text{C}_{15}\text{ZnO}$ be around oxygen atom, zinc atom and some carbon atoms. The charge concentration in the nanomaterial structures $\text{Li}_{15}\text{C}_{15}\text{FeS}_2$ be around disulfur atoms and some carbon atoms. The concentration charge in the regions near carbon, zinc, oxygen and disulfur atoms denotes to occur adsorption phenomena.

2.4. Infrared Spectra (IR)

The stretching vibrations can be classified as either symmetrical or asymmetrical. When atoms oscillate in the same phase, stretching vibrations take place. When the atoms oscillate with various phases, this leads to non-stretching vibrations. Harmonic vibrational frequencies are provided using infrared spectroscopy. There are two types of vibration modes: inelastic and elastic [3, 22]. The electronic density contours for the nanomaterials $\text{Li}_{10}\text{C}_{10}$, $\text{Li}_{10}\text{C}_{10}\text{ZnO}$, $\text{Li}_{10}\text{C}_{10}\text{FeS}_2$, $\text{Li}_{15}\text{C}_{15}$, $\text{Li}_{15}\text{C}_{15}\text{ZnO}$ and $\text{Li}_{15}\text{C}_{15}\text{FeS}_2$. DFT have been carried out throughout utilizing density functional theory (DFT) with the hybrid functional B3LYP and the basis set 6-31G at the ground state level.

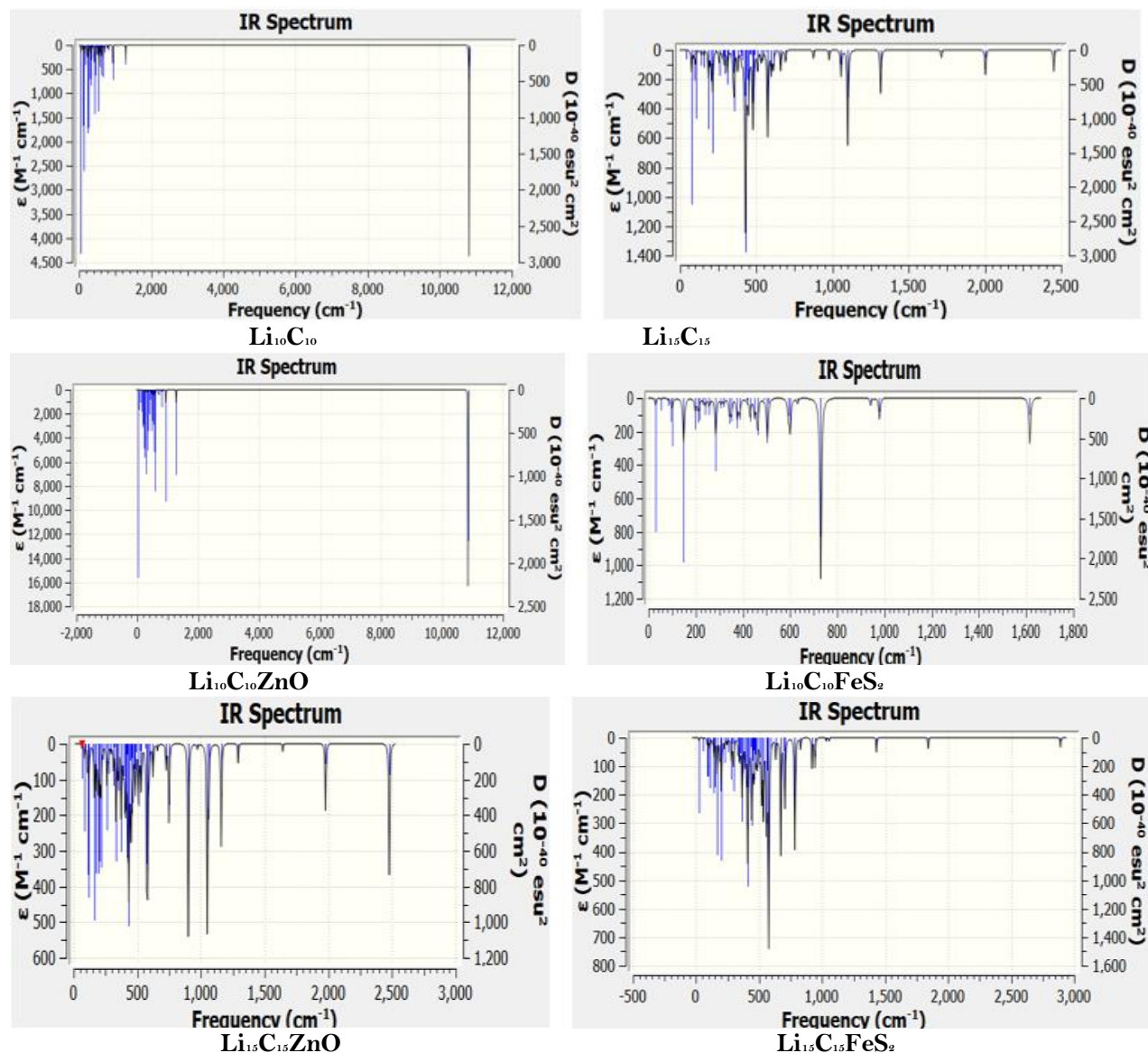


Figure 4.

The infrared spectra (IR) for $\text{Li}_{10}\text{C}_{10}$, $\text{Li}_{10}\text{C}_{10}\text{ZnO}$, $\text{Li}_{10}\text{C}_{10}\text{FeS}_2$, $\text{Li}_{15}\text{C}_{15}$, $\text{Li}_{15}\text{C}_{15}\text{ZnO}$ and $\text{Li}_{15}\text{C}_{15}\text{FeS}_2$.

Figure 4 shows a new apex originate after the adsorption procedure of zinc oxide on the nanomaterial surfaces $\text{Li}_{10}\text{C}_{10}$ and $\text{Li}_{15}\text{C}_{15}$, also a new apex originate after the adsorption procedure of iron disulfide on the nanomaterial surfaces $\text{Li}_{10}\text{C}_{10}$ and $\text{Li}_{15}\text{C}_{15}$. The apexes in the infrared spectra indicates to formation new bonds like (Zn-Li), (Zn-C), (Fe-Li) and (Fe-C). Before the adsorption procedure of ZnO on the nanomaterial surface $\text{Li}_{10}\text{C}_{10}$ the apex between (10000-12000) cm^{-1} demonstrates at intensity close to (4500 $\text{mole}^{-1}\text{cm}^{-1}$), but after the adsorption procedure of ZnO on the nanomaterial surface $\text{Li}_{10}\text{C}_{10}$ the apex between (10000-12000) cm^{-1} becomes at intensity close to (12500 $\text{mole}^{-1}\text{cm}^{-1}$). The adsorption procedure of FeS_2 on the nanomaterial surface $\text{Li}_{10}\text{C}_{10}$ leads to shielding procedure. One can visualize the shielding procedure clearly throughout disappearing the clear peak between (10000-12000) cm^{-1} in $\text{Li}_{10}\text{C}_{10}\text{FeS}_2$, whereas, the peaks was existing in the nanomaterial surface $\text{Li}_{10}\text{C}_{10}$. The shielding procedure generally obtains because of tendency of the atoms in FeS_2 to interact with some atoms more

than other atoms. Tentatively infrared spectroscopy can be achieved through special diagnostics devices in chemistry laboratories. Infrared spectra explain bonding nature and strength bonding in the molecular structures.

2.5. Electronic States and Energy Gap (E_g)

With accordance to molecular orbital theory the atomic orbitals are combined linearly to create the molecular orbitals. The energy gap (E_g) is the difference between HOMO energy and LUMO energy. The energy gap (E_g) is very important merit in the physics of solids. With accordance to the energy gap (E_g) merit, it can be distinguished among the materials I they are insulators, semiconductors or conductors. Mathematically the energy gap (E_g) can be calculated by utilizing the equation [23, 24].

$$E_g = E_{LUMO} - E_{HOMO} \quad \dots (1)$$

Table 1.

Summarizes HOMO, LUMO energies and energy gaps for $\text{Li}_{10}\text{C}_{10}$, $\text{Li}_{10}\text{C}_{10}\text{ZnO}$, $\text{Li}_{10}\text{C}_{10}\text{FeS}_2$, $\text{Li}_{15}\text{C}_{15}$, $\text{Li}_{15}\text{C}_{15}\text{ZnO}$ and $\text{Li}_{15}\text{C}_{15}\text{FeS}_2$.

System	$E_{HOMO}(\text{eV})$	$E_{LUMO}(\text{eV})$	$E_g(\text{eV})$
$\text{Li}_{10}\text{C}_{10}$	-3.8899416	-3.3212526	0.568689
$\text{Li}_{10}\text{C}_{10}\text{ZnO}$	-4.8085512	-4.1691162	0.639435
$\text{Li}_{10}\text{C}_{10}\text{FeS}_2$	-3.9914349	-3.191733	0.799702
$\text{Li}_{15}\text{C}_{15}$	-3.8254539	-3.148197	0.677257
$\text{Li}_{15}\text{C}_{15}\text{ZnO}$	-3.7952508	-2.9620806	0.83317
$\text{Li}_{15}\text{C}_{15}\text{FeS}_2$	-4.1677557	-3.1016679	1.066088

Table 1 demonstrates that the energy gap of each nanomaterial in the range of energy gap of semiconductors. This values of energy gap E_g are tremendously beneficial in the manufacture of electronic devices. One can visualize that the nanomaterial $\text{Li}_{15}\text{C}_{15}$ has energy gap close to the energy gap of germanium, $E_g(\text{Ge})=0.67$ eV, one can say this value of energy gap to the nanomaterial $\text{Li}_{15}\text{C}_{15}$ can be consider very beneficial in the semiconductor applications, such as , solid state lasers, p-n junctions, solar cells, optoelectronics and microelectronic circuits. The adsorption procedure of ZnO on the nanomaterial surface $\text{Li}_{15}\text{C}_{15}$ leads to increase the value of energy gap to become close to the energy gap of gallium antimony, $E_g(\text{GaSb})=0.81$ eV. This value of energy gap is very important in the photovoltaic systems and transistors. HOMO or SOMO energies links to trend the nanomaterial structure for donation the electrons from, whether, LUMO energy links to trend the nanomaterial structure for acceptance the electrons. The big values of HOMO or SOMO means high tendency of the nanomaterial structure to donate the electrons. The small value LUMO means strong tendency of the nanomaterial structure to accept electrons.

2.6. Polarizability

The term polarizability indicates to a molecule's capacity for polarization. The polarizability typifies a second order variation in the energy, it establishes the linear response of the electron density in the presence of an infinite fundamental electric field F [25].

$$\alpha = -\left(\frac{\partial^2}{\partial F_a \partial F_b}\right)_{a,b} = x, y, z \quad (2)$$

The polarizability tensors Eigen values α_{xx} , α_{yy} and α_{zz} are the quantities that determine the valueof average polarizability according to the mathematical equation [6].

$$\langle \alpha \rangle = \frac{1}{3}(\alpha_{xx} + \alpha_{yy} + \alpha_{zz}) \quad (3)$$

Table 2.Summarizes average polarizabilities $\langle \alpha \rangle$ for $\text{Li}_{10}\text{C}_{10}$, $\text{Li}_{10}\text{C}_{10}\text{ZnO}$, $\text{Li}_{10}\text{C}_{10}\text{FeS}_2$, $\text{Li}_{15}\text{C}_{15}$, $\text{Li}_{15}\text{C}_{15}\text{ZnO}$ and $\text{Li}_{15}\text{C}_{15}\text{FeS}_2$.

System	$\langle \alpha \rangle$ (a.u)
$\text{Li}_{10}\text{C}_{10}$	808.571427
$\text{Li}_{10}\text{C}_{10}\text{ZnO}$	765.864019
$\text{Li}_{10}\text{C}_{10}\text{FeS}_2$	940.745591
$\text{Li}_{15}\text{C}_{15}$	1327.898844
$\text{Li}_{15}\text{C}_{15}\text{ZnO}$	1372.449218
$\text{Li}_{15}\text{C}_{15}\text{FeS}_2$	1311.425613

Table 2 demonstrates that the nanomaterial structure ($\text{Li}_{15}\text{C}_{15}\text{ZnO}$) is the highest activity nanomaterial structure in the table since it possesses the maximum numerical value of the average polarizability $\langle \alpha \rangle$, it equals to (1372.449218 a.u). The average polarizability merit is considered very advantageous, the reason here, it provides information about the internal structure and the dipole moment without holding calculations. The average polarizability merit has importance in the science of nonlinear optics. The polarizability property determines the electronic charge distribution in the molecular structure. One can visualize that influence the average polarizabilities randomly, that is to say, the adsorption procedure of ZnO on the nanomaterial surface $\text{Li}_{10}\text{C}_{10}$ causes decreasing the value of average polarizability from approximately (808.57 a.u) to (765.86 a.u), but the adsorption procedure of ZnO on the nanomaterial surface causes increasing the value of average polarizability from approximately (1327.89 a.u) to (1372.44 a.u). The interpretation of this random impact of the adsorption is the constrains o quantum mechanics and Fermi-Dirac distribution. The electrons movement in the molecular structure be restricted by Fermi-Dirac distribution.

2.7. Ionization Potential and Electron Affinity

Ionization potential (I.P) is expressed by the first ionization energy of the atom. The ionization energy stands for minimum energy requires to convert one mole o the atom in the gaseous state (stationary state that has lowest energy) into one mole of the unipolar charge gaseous ion. The electron affinity (E.A) describes the variation in the binding energy. The electron affinity can be defined as the variation in the internal energy which gets when one mole of atom in the gaseous state converts by acquisition an electron to get one mole of the negative ions in gaseous state [26, 27]. According to Koopman's theorem ionization potentials (I.Ps) and electron affinities (E.As) can be founded from the equations [28].

$$E_{\text{HOMO}} = -I.P \quad (4)$$

$$E_{\text{LUMO}} = -E.A \quad (5)$$

Table 3.Ionization potential and electron affinity for $\text{Li}_{10}\text{C}_{10}$, $\text{Li}_{10}\text{C}_{10}\text{ZnO}$, $\text{Li}_{10}\text{C}_{10}\text{FeS}_2$, $\text{Li}_{15}\text{C}_{15}$, $\text{Li}_{15}\text{C}_{15}\text{ZnO}$ and $\text{Li}_{15}\text{C}_{15}\text{FeS}_2$.

System	I.P(eV)	E.A(eV)
$\text{Li}_{10}\text{C}_{10}$	3.8899416	3.3212526
$\text{Li}_{10}\text{C}_{10}\text{ZnO}$	4.8085512	4.1691162
$\text{Li}_{10}\text{C}_{10}\text{FeS}_2$	3.9914349	3.191733
$\text{Li}_{15}\text{C}_{15}$	3.8254539	3.148197
$\text{Li}_{15}\text{C}_{15}\text{ZnO}$	3.7952508	2.9620806
$\text{Li}_{15}\text{C}_{15}\text{FeS}_2$	4.1677557	3.1016679

Table 3 provides a summary of the electron affinities and ionization potential values before and after the adsorption procedure of zinc oxide and iron sulfide on the nanomaterial surfaces $\text{Li}_{10}\text{C}_{10}$ and $\text{Li}_{15}\text{C}_{15}$. The adsorption of ZnO on the nanomaterial surface $\text{Li}_{15}\text{C}_{15}$ make the new nanomaterial structure $\text{Li}_{15}\text{C}_{15}\text{ZnO}$ has the lowest ionization potential value, which is roughly (3.7952508 eV). The adsorption procedure of ZnO on the nanomaterial surface ($\text{Li}_{10}\text{C}_{10}$) make it the best acceptor because it has the maximum value electron affinity, which is roughly (4.1691162 eV). The ionization potentials and

electron affinities are considered very advantageous in determination another important properties, just like chemical potential, softness, electrophilicity and hardness. The strength of donation of the electrons from HOMO or SOMO level is measured by the ionization potential (I.P), the energy release by donation electron from HOMO or SOMO level. The strength of acceptance of the electrons in LUMO level is measured by the electron affinity (E.A), the energy release by acceptance electrons in LUMO level. The Ionization potential property has great advantage, it predicts to the stability of the nanomaterial structures. The electron affinity property has great advantage, it predicts to the electronic chemical potential of the nanomaterial structures.

2.8. Dipole Moment

The result of multiplication the charge by the displacement is the dipole moment. The dipole moment originates between two charges which are separated by a straight distance (r). The dipole moment varies when the displacement varies in any direction. Let μ typifies the electric dipole moment, q typifies the charge and r typifies the displacement between two charges, therefore, the dipole moment can be expressed by the equation [29].

$$\mu = q * r \quad \dots (6)$$

Table 4.

Summarizes dipole moments in (Debye) for $\text{Li}_{10}\text{C}_{10}$, $\text{Li}_{10}\text{C}_{10}\text{ZnO}$, $\text{Li}_{10}\text{C}_{10}\text{FeS}_2$, $\text{Li}_{15}\text{C}_{15}$, $\text{Li}_{15}\text{C}_{15}\text{ZnO}$ and $\text{Li}_{15}\text{C}_{15}\text{FeS}_2$.

System	Dipole moment (Debye)
$\text{Li}_{10}\text{C}_{10}$	16.614428
$\text{Li}_{10}\text{C}_{10}\text{ZnO}$	25.939414
$\text{Li}_{10}\text{C}_{10}\text{FeS}_2$	20.148867
$\text{Li}_{15}\text{C}_{15}$	17.590756
$\text{Li}_{15}\text{C}_{15}\text{ZnO}$	23.898089
$\text{Li}_{15}\text{C}_{15}\text{FeS}_2$	26.456102

Table 4 clarifies impact of the adsorption procedure of zinc oxide and iron disulfide to the values of dipole moments of the nanomaterial surfaces $\text{Li}_{10}\text{C}_{10}$ and $\text{Li}_{15}\text{C}_{15}$, the adsorption procedure leads to apparent increasing in the values of dipole moment of the nanomaterials after the adsorption. The nanomaterial structure ($\text{Li}_{15}\text{C}_{15}\text{FeS}_2$) is the highest dipole moment, it has value of dipole moment equal to (26.456102 Debye). The dipole moment merit connect to the bond strength, charge density and polarizability. The dipole moment merit reveals the separate distance among the charges in the molecular structure. The dipole moment of the nanomaterial structures depend dramatically on the electronegativity of the interacting materials. One of the most impact parameters on the dipole moment is the symmetry. The dipole moment play an active role in the molecular structure, it determines the polarity o the covalent bond. The dipole moment measure the bond strength and charge density in the chemical structure. The large dipole moment materials have advantage for creating materials have high dielectric constant, which is advantageous in the capacitors.

2.9. Symmetry

The mathematical group consists of number of elements that linked with accordance to determined rules. The particular kind that links to the symmetry of molecules is the symmetry elements. There is a symmetry operation accompany each symmetry element. Generally, there are seven elements of the symmetry, they are: identity, horizontal axis, vertical plane, dihedral plane, improper axis, proper axis and inversion center or center of symmetry [30, 31].

Table 5.Summarizes point group symmetries for $\text{Li}_{10}\text{C}_{10}$, $\text{Li}_{10}\text{C}_{10}\text{ZnO}$, $\text{Li}_{10}\text{C}_{10}\text{FeS}_2$, $\text{Li}_{15}\text{C}_{15}$, $\text{Li}_{15}\text{C}_{15}\text{ZnO}$ and $\text{Li}_{15}\text{C}_{15}\text{FeS}_2$.

System	Point group symmetry
$\text{Li}_{10}\text{C}_{10}$	C_s/C_1
$\text{Li}_{10}\text{C}_{10}\text{ZnO}$	C_s/C_1
$\text{Li}_{10}\text{C}_{10}\text{FeS}_2$	C_1
$\text{Li}_{15}\text{C}_{15}$	C_1
$\text{Li}_{15}\text{C}_{15}\text{ZnO}$	C_1
$\text{Li}_{15}\text{C}_{15}\text{FeS}_2$	C_1

Table 5 demonstrates that the adsorption procedure of iron disulfide on the nanomaterial surface ($\text{Li}_{10}\text{C}_{10}$) make it has the symmetry C_1 rather than C_s/C_1 . The symmetry operation C_s leave the nanomaterial structure alone, the symmetry element here is identity. Although the symmetry operation C_s let the nanomaterial structure it's same without any variation, but this symmetry operation is necessary for the group theoretically. It express on some operations such as the double reflection of the nanomaterial structure in the symmetry plane. The symmetry operation C_1 of the nanomaterial structures in the table belong to the symmetry operation of the type C_n , the symmetry element here is proper axis. The point group symmetry C_n results from rotates the nanomaterial structure by 360° , one can say the nanomaterial structure will belong the same after complete cycle because ($n=1$) and the rotation occurs at ($360^\circ/n$). The symmetry property considers importance property, it impact to the molecular structure, reaction mechanics dipole moment and degenerate states. Symmetry considers advantageous in optical activity of the compounds.

2.10. Density of States (DOS)

The density of states express on the number of states per unit energy. The density of states merit contributes to interpretation many of physics phenomena, especially solid state physics. The density of state at Fermi level has greater importance to know the merits of minerals, just like, specific heat. The density of state depends on the effective mass according to quantum physics ideas [7, 32]. The density of states (DOS) for the nanomaterials $\text{Li}_{10}\text{C}_{10}$, $\text{Li}_{10}\text{C}_{10}\text{ZnO}$, $\text{Li}_{10}\text{C}_{10}\text{FeS}_2$, $\text{Li}_{15}\text{C}_{15}$, $\text{Li}_{15}\text{C}_{15}\text{ZnO}$ and $\text{Li}_{15}\text{C}_{15}\text{FeS}_2$. DFT have been carried out throughout utilizing density functional theory (DFT) with the hybrid functional B3LYP and the basis set 6-31G at the ground state level.

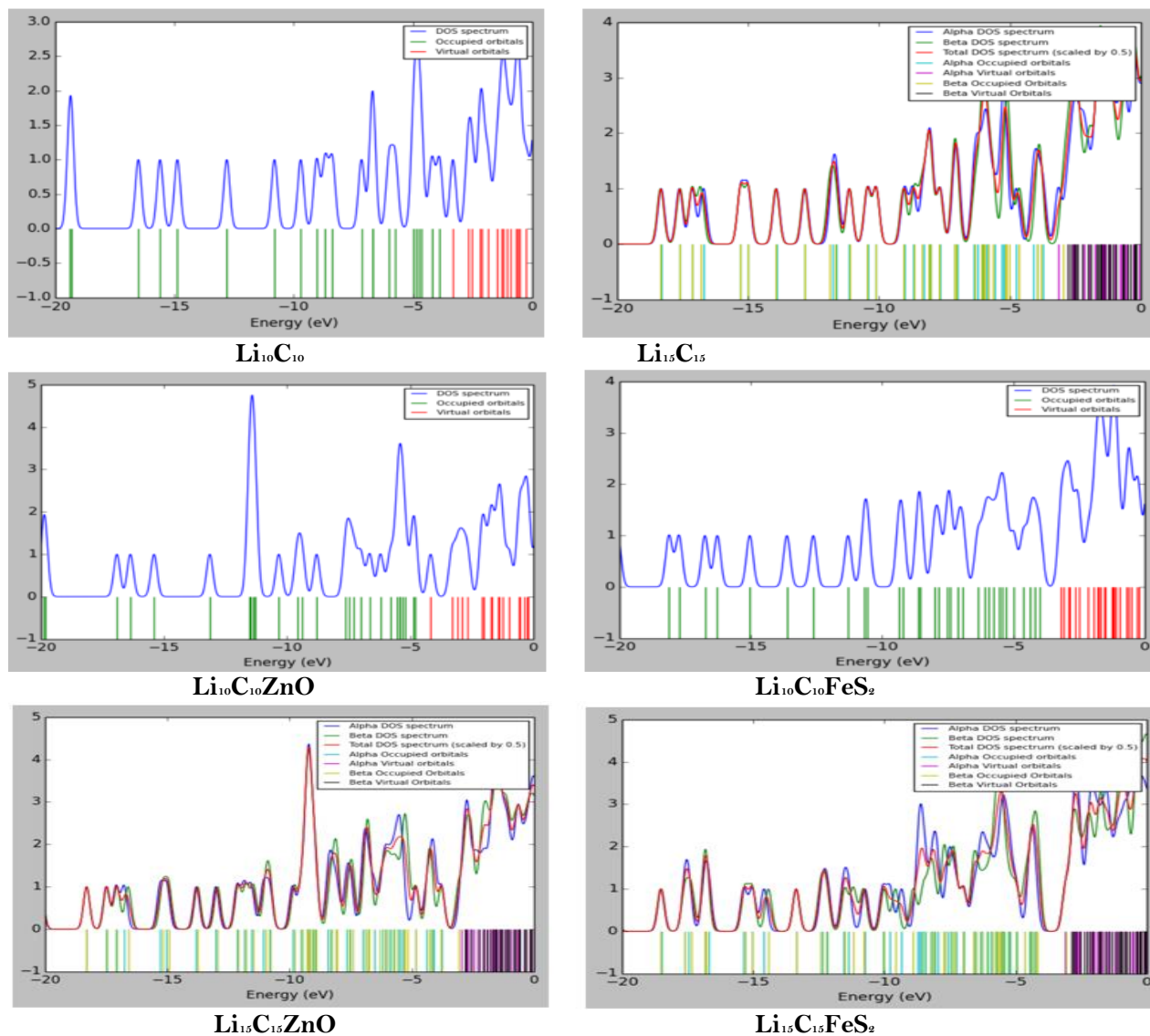


Figure 5. The density of states (DOS) for $\text{Li}_{10}\text{C}_{10}$, $\text{Li}_{10}\text{C}_{10}\text{ZnO}$, $\text{Li}_{10}\text{C}_{10}\text{FeS}_2$, $\text{Li}_{15}\text{C}_{15}$, $\text{Li}_{15}\text{C}_{15}\text{ZnO}$ and $\text{Li}_{15}\text{C}_{15}\text{FeS}_2$.

Figure 5 demonstrates the nanomaterial structures $\text{Li}_{15}\text{C}_{15}$, $\text{Li}_{15}\text{C}_{15}\text{ZnO}$ and $\text{Li}_{15}\text{C}_{15}\text{FeS}_2$ as anti-ferromagnetic nanomaterials because they have two dissimilar types of orbitals: alpha (α) and beta (β). The anti-ferromagnetic property means small and positive magnetism ability. The anti-ferromagnetic is advantageous in the manufacture of sensors. The adsorption procedure of ZnO on the nanomaterial surface $\text{Li}_{10}\text{C}_{10}$ leads to origination new energetic states which can be occupied with electrons. Before the adsorption procedure the nanomaterial surface $\text{Li}_{10}\text{C}_{10}$ at the energy close (-13 eV) the density of state equal to (1), but after the adsorption procedure the nanomaterial structure $\text{Li}_{10}\text{C}_{10}\text{ZnO}$ had density of state close to (5). Either new energetic states demonstrate as a result to adsorption procedure of iron disulfide on the nanomaterial surface $\text{Li}_{10}\text{C}_{10}$. The density of state diagrams help to determine if the material consider metal or non-metal or semiconductor, it determine the available energetic levels according to Fermi-Dirac distribution. Density of state depend dramatically on the effective mass of the electrons, density of state increase as the effective mass increase. The density of states property

contribute to understand the electronic properties of the materials and specific heat of the substances. The nanomaterial structures $\text{Li}_{15}\text{C}_{15}$, $\text{Li}_{15}\text{C}_{15}\text{ZnO}$ and $\text{Li}_{15}\text{C}_{15}\text{FeS}_2$ own anti-ferromagnetic merit.

3. Conclusions

The molecular structure at 6-31G and B3LYP basis sets could be accomplished with quintessential algorithms in Gaussian09 program for carbon lithium nanomaterial surfaces and the adsorption procedure of zinc oxide and iron disulfide on the nanomaterial surfaces $\text{Li}_{10}\text{C}_{10}$ and $\text{Li}_{15}\text{C}_{15}$. The electrostatic potential surfaces and contour density maps demonstrate that distribution of the electronic charges about the atoms impact dramatically to the adsorption procedure. Infrared spectra diagrams demonstrate occurring shielding procedure when FeS_2 interacts with the nanomaterial surface $\text{Li}_{10}\text{C}_{10}$, the shielding procedure gets because trend of atoms in iron disulfide (FeS_2) to interact with some atoms more than other atoms. The energy gap of the nanomaterial nanostructure $\text{Li}_{15}\text{C}_{15}$ closes to the energy gap of germanium $E_g(\text{Ge})=0.67$ eV, this value of energy gap owns advantage in the semiconductor devices industries such as semiconductor laptop pieces. The nanomaterial structure ($\text{Li}_{15}\text{C}_{15}\text{ZnO}$) is the biggest vitality nanomaterial structure in this treatise as it owns the maximum value of the average polarizability ($\langle\alpha\rangle = 1372.449218$ a.u). The polarizability credit be considered advantageous, it supplies information about the internal structure and the dipole moment without holding calculations, polarizability merit is one of the merit that involve the nonlinear phenomena. The adsorption procedure of ZnO on the nanomaterial surface ($\text{Li}_{10}\text{C}_{10}$) make it the best acceptor because it has the greatest value electron affinity, which is roughly (4.1691162 eV). The adsorption of ZnO on the nanomaterial surface $\text{Li}_{15}\text{C}_{15}$ makes the new nanomaterial structure $\text{Li}_{15}\text{C}_{15}\text{ZnO}$ has the minimum ionization potential value, which is roughly (3.7952508 eV), this makes $\text{Li}_{15}\text{C}_{15}\text{ZnO}$ the optimal donor in this treatise. The nanomaterial structure ($\text{Li}_{15}\text{C}_{15}\text{FeS}_2$) is the maximum dipole moment nanomaterial structure, it equals to (26.456102 Debye). The large dipole moment nanomaterials own an importance for creating nanomaterials own high dielectric constant, which is beneficial in the capacitors industry. The adsorption procedure of iron disulfide on the nanomaterial surface ($\text{Li}_{10}\text{C}_{10}$) make it owns the symmetry C_1 instead of C_s/C_1 . Symmetry play a vital role to determine the optical activity of the compounds. The adsorption procedure of iron disulfide on the nanomaterial surface $\text{Li}_{10}\text{C}_{10}$ leads to appearance new energetic levels can be occupied by electrons. The nanomaterial structures $\text{Li}_{15}\text{C}_{15}$, $\text{Li}_{15}\text{C}_{15}\text{ZnO}$ and $\text{Li}_{15}\text{C}_{15}\text{FeS}_2$ own have two dissimilar kinds of orbitals: alpha (α) and beta (β) therefore, they are anti-ferromagnetic nanomaterials. The anti-ferromagnetic materials own importance in the sensors devices.

Transparency:

The authors confirm that the manuscript is an honest, accurate, and transparent account of the study; that no vital features of the study have been omitted; and that any discrepancies from the study as planned have been explained. This study followed all ethical practices during writing.

Acknowledgements:

The authors would like to thank the Physics Department, College of science, Thi-Qar University, Thi-Qar, Iraq.

Copyright:

© 2025 by the authors. This open-access article is distributed under the terms and conditions of the Creative Commons Attribution (CC BY) license (<https://creativecommons.org/licenses/by/4.0/>).

References

- [1] M. H. Assadi and D. A. Hanaor, "Theoretical study on copper's energetics and magnetism in TiO_2 polymorphs," *Journal of Applied Physics*, vol. 113, no. 23, pp. 234105-234110, 2013. <https://doi.org/10.1063/1.4802879>
- [2] G. Vignale and M. Rasolt, "Density-functional theory in strong magnetic fields," *Physical Review Letters*, vol. 59, no. 20, pp. 2360-2363, 1987. <https://doi.org/10.1103/PhysRevLett.59.2360>

- [3] M. K. Hommod and L. F. Auqla, "Density functional theory investigation for Ni6, Co5, Au12, Y5 and Ni6Li, Co5Li, Au12Li, Y5Na interactions," *University of Thi-Qar Journal of Science*, vol. 9, no. 2, pp. 105-112, 2022.
- [4] P. Rg and W. Yang, *Density-functional theory of atoms and molecules*. New York: Oxford University Press, 1989.
- [5] W. Koch and M. C. Holthausen, *A chemist's guide to density functional theory*, 3rd ed. Hoboken, NJ: John Wiley & Sons, 2015.
- [6] A. M. Ali, "Investigations of some antioxidant materials by using density functional and semiempirical theories," P. HD. Thesis, University of Basrah, College of Science, Department of Physics, 2009.
- [7] C. Kittel and P. McEuen, *Introduction to solid state physics*, 9th ed. Hoboken, NJ: John Wiley & Sons, 2018.
- [8] S. Grimme, "Semiempirical hybrid density functional with perturbative second-order correlation," *The Journal of Chemical Physics*, vol. 124, no. 3, p. 034108, 2006. <https://doi.org/10.1063/1.2136180>
- [9] C. J. Carmer, *Essentials of computational chemistry*. Chichester: John Wiley & Sons, Ltd, 2002.
- [10] G. G. Amatucci, F. Badway, A. Du Pasquier, and T. Zheng, "An asymmetric hybrid nonaqueous energy storage cell," *Journal of the Electrochemical Society*, vol. 148, no. 8, pp. A930-A937, 2001. <https://doi.org/10.1149/1.1378109>
- [11] J. Ajuria, E. Redondo, M. Arnaiz, R. Mysyk, T. Rojo, and E. Goikolea, "Lithium and sodium ion capacitors with high energy and power densities based on carbons from recycled olive pits," *Journal of Power Sources*, vol. 359, pp. 17-26, 2017. <https://doi.org/10.1016/j.jpowsour.2017.04.067>
- [12] J. Ding, W. Hu, E. Paek, and D. Mitlin, "Review of hybrid ion capacitors: From aqueous to lithium to sodium," *Chemical Reviews*, vol. 118, no. 14, pp. 6457-6498, 2018. <https://doi.org/10.1021/acs.chemrev.8b00173>
- [13] Á. Doñoro, D. Cíntora-Juárez, and V. Etacheri, "Carbon nanomaterials for rechargeable lithium-sulfur batteries. In Carbon Based Nanomaterials for Advanced Thermal and Electrochemical Energy Storage and Conversion," Elsevier. <https://doi.org/10.1016/B978-0-12-813424-7.00017-4>, 2019, pp. 279-309.
- [14] Y. Zhang, Y. Jiao, M. Liao, B. Wang, and H. Peng, "Carbon nanomaterials for flexible lithium ion batteries," *Carbon*, vol. 124, pp. 79-88, 2017. <https://doi.org/10.1016/j.carbon.2017.08.022>
- [15] Y. Wang, Y. Song, and Y. Xia, "Electrochemical capacitors: mechanism, materials, systems, characterization and applications," *Chemical Society Reviews*, vol. 45, no. 21, pp. 5925-5950, 2016. <https://doi.org/10.1039/C6CS00355C>
- [16] R. J. Gillespie, *Molecular geometry*. New York: Van Nostrand Reinhold, 1972.
- [17] A. S. Alwan, S. K. Ajeel, and M. L. Jabbar, "Theoretical study for coronene and Coronene-Al, B, C, Ga, In and Coronene-O interactions by using density functional theory," *University of Thi-Qar Journal*, vol. 14, no. 4, pp. 1-14, 2019.
- [18] F. Thamer and A. Shwya, "Theoretical study of physisorption of tosylate on AU10, AU15 and AU18 surfaces utilizing DFT approach," *Nexo Revista Científica*, vol. 36, no. 06, pp. 968-982, 2023.
- [19] M. J. Frisch, G. W. Trucks, H. B. Schlegel, and G. E. Scuseria, *Gaussian 09*. Wallingford, CT: Gaussian, Inc, 2009.
- [20] A. B. Ahmed, "Studying the electronic characteristics and physisorption of OTS on the pure silver surfaces (Ag10),(Ag15) and (Ag18)," *University of Thi-Qar Journal of Science*, vol. 10, no. 2, pp. 151-159, 2023.
- [21] S. H. Talib and A. S. Alwan, "Geometrical optimization and some electrical properties for pyrrole-metal interactions using DFT, B3LYP basis sets," *Journal of Optoelectronics Laser*, vol. 41, no. 7, pp. 1300-1312, 2022.
- [22] M. K. AL-Khaykane and H. I. Aboud, "Study of the electronic properties for di-amino naphthalene: B3LYP density functional theory calculations," *International Journal of Pure and Applied Sciences and Technology*, vol. 15, no. 1, pp. 1-13, 2013.
- [23] M. L. Jabbar, "Some electrical properties for Coronene-Y interactions by using density functional theory (DFT)," *Journal of Basrah Researches ((Sciences))*, vol. 44, no. 1, pp. 1-9, 2018.
- [24] S. M. Sze, *Semiconductor devices: Physics and technology*. New York: John Wiley & Sons, 2008.
- [25] J. P. Inchaustegui and R. Pumachagua, "Computational study on second-order nonlinear optical properties of donor-acceptor substituted copper phthalocyanines," *Revista de la Sociedad Química del Perú*, vol. 81, no. 3, pp. 232-241, 2015. <https://doi.org/10.26439/rsqp2015.v081n3.3890>
- [26] J. Barrett, *Structure and bonding*. Cambridge, UK: Royal Society of Chemistry, 2001.
- [27] J. Barrett, *Atomic structure and periodicity*. Cambridge, UK: Royal Society of Chemistry, 2002.
- [28] L. W. Beck, T. Xu, J. B. Nicholas, and J. F. Haw, "Kinetic NMR and density functional study of benzene H/D exchange in zeolites, the most simple aromatic substitution," *Journal of the American Chemical Society*, vol. 117, no. 46, pp. 11594-11595, 1995. <https://doi.org/10.1021/ja00147a050>
- [29] H. M. Jawad, T. A. Husain, and I. N. Qader, "Study of physical and electrical properties of sandwich compound as drug delivery to transport chlorpheniramine medication using density functional theory," *Journal of Physical Chemistry and Functional Materials*, vol. 6, no. 2, pp. 124-131, 2023.
- [30] D. M. Bishop, *Group theory and chemistry*. Mineola, NY: Dover Publications: , 1993.
- [31] A. M. Lesk, *Introduction to symmetry and group theory for chemists*. New York: Springer, 2004.
- [32] J. Honig, *Solid state physics (Blakemore, J. S.)*. Washington, D.C: ACS Publications, 1970.